

This is the accepted manuscript made available via CHORUS. The article has been published as:

Modular matrices from universal wave-function overlaps in Gutzwiller-projected parton wave functions

Jia-Wei Mei and Xiao-Gang Wen

Phys. Rev. B **91**, 125123 — Published 12 March 2015

DOI: [10.1103/PhysRevB.91.125123](https://doi.org/10.1103/PhysRevB.91.125123)

Modular matrices from universal wave function overlaps in Gutzwiller-projected parton wave functions

Jia-Wei Mei¹ and Xiao-Gang Wen^{2,1}

¹*Perimeter Institute for Theoretical Physics, Waterloo, Ontario, N2L 2Y5 Canada*

²*Department of Physics, Massachusetts Institute of Technology, Cambridge, Massachusetts 02139, USA*

(Dated: February 23, 2015)

We implement the universal wave function overlap (UWFO) method to extract modular S and T matrices for topological orders in Gutzwiller-projected parton wave functions (GPWFs). The modular S and T matrices generate a projective representation of $SL(2, \mathbb{Z})$ on the degenerate-ground-state Hilbert space on a torus and may fully characterize the 2+1D topological orders, i.e. the quasi-particle statistics and chiral central charge (up to E_8 bosonic quantum Hall states). We use the variational Monte Carlo method to compute the S and T matrices of the chiral spin liquid (CSL) constructed by the GPWF on the square lattice, and confirm that the CSL carries the same topological order as the $\nu = \frac{1}{2}$ bosonic Laughlin state. We find that the non-universal exponents in UWFO can be small and direct numerical computation is able to be applied on relatively large systems. UWFO may be a powerful method to calculate the topological order in GPWFs.

Topological order¹⁻³ connotes the pattern of long-range entanglement in gapped many-body wave functions⁴⁻⁶. It describes gapped quantum phases of matter that lie beyond the Landau symmetry breaking paradigm⁷. Local unitary transformations on many-body wave functions can remove local entanglement, however, preserve the long-range topological entanglement. Therefore, a topological ordered state is not smoothly connected to a trivial (direct product) state by local unitary transformations⁶. Physically, topological order is described through topological quantum numbers, such as non-trivial ground state structures and fractional excitations.^{1-3,8-10} These topological properties are fully characterized by the quasi-particle (anyon in the bulk) statistics⁸⁻¹⁰ and the chiral central charge which encodes information about chiral gapless edge states^{11,12}.

Both the fusion rule and the topological spin of quasi-particles as well as the chiral central charge are characterized in the non-Abelian geometric phases encoded in the degenerate ground states^{1-3,13-17}, and vice versa. The non-Abelian geometric phases form a representation of $SL(2, \mathbb{Z})$, that is generated by 90° rotation and Dehn twist on a torus, which are called modular S and T matrices, respectively^{13,14}. The element of the modular S matrix determines the mutual statistics of quasi-particles while the element of the T matrix determines the topological spin $\theta_a \in U(1)$ and the chiral central charge^{1,13,14}.

Given the fusion coefficients N_c^{ab} and the topological spin θ_a , we can write down the modular S and T matrices as the following expressions, $S_{ab} = \frac{1}{\mathcal{D}} \sum_c N_c^{ab} \frac{\theta_c}{\theta_a \theta_b} d_c$ and $T_{ab} = e^{-i \frac{2\pi c}{24} \theta_a} \delta_{a,b}$.¹⁸ Here d_a (called the quantum dimension of quasiparticle a) is the largest eigenvalue of matrix N_a which is defined as $(N_a)_{bc} = N_c^{ab}$ and \mathcal{D} is the total quantum dimension, $\mathcal{D}^2 = \sum_a d_a^2$. We see that $S_{a1} = \frac{d_a}{\mathcal{D}}$.

From Verlinde formula¹⁹, we can reconstruct the fusion coefficients, $N_{ab}^c = \sum_x \frac{S_{ax} S_{bx} S_{cx}^*}{S_{1x}}$. Therefore, S and T provide a complete description and can be taken as the order parameter of topological orders¹⁴⁻¹⁷. The modular

S and T matrices satisfy the relations, $(ST)^3 = C$ and $S^2 = C$, where C is a so-called charge conjugation matrix that satisfies $C^2 = 1$. The central charge c determines the thermal current of the edge state, $I_E = \frac{c}{6} T^2$, at temperature T ²⁰ and is fixed up to E_8 bosonic quantum Hall states.

To fully characterize topological order, various numerical methods are proposed to access the modular S and T matrices from ground state wave functions²¹⁻²⁶. By braiding quasiholes, the modular S and T can be extracted from the berry matrices.²⁷⁻²⁹ Recently, one of us proposed the universal wave function overlap (UWFO) method to calculate modular matrices^{16,30}. For a given set $\{|\psi_a\rangle\}_{a=1}^N$ of degenerate ground-state wave functions, it provides us a practical method to extract the modular S and T matrices

$$\begin{aligned}\tilde{S}_{ab} &= \langle \psi_a | \hat{S} | \psi_b \rangle = e^{-\alpha_S L^2 + o(1/L^2)} S_{ab}, \\ \tilde{T}_{ab} &= \langle \psi_a | \hat{T} | \psi_b \rangle = e^{-\alpha_T L^2 + o(1/L^2)} T_{ab},\end{aligned}\quad (1)$$

where \hat{S} and \hat{T} are the operators that generate the 90° rotation and Dehn twist, respectively, on a torus with the L^2 lattice size. The exponentially small prefactor makes it difficult to numerically calculate the UWFO in (1). To avoid the exponential smallness, a gauge-symmetry preserved tensor renormalization method has been developed for the tensor-network wave functions^{16,17}, where the system size is effectively reduced as zero after the tensor renormalization.

Actually, in this paper, we will show that the non-universal exponent $\alpha_{T,S}$ can be small such that the UWFO can be directly numerically calculated on relatively large systems. We will take a chiral spin liquid (CSL) wave function on the square lattice³¹ as an explicit example to extract the modular S and T matrices from the UWFO. We construct the set of the ground states for a CSL by using Gutzwiller-projected parton wave functions (GPWF).^{21,31-34} We use the variational Monte Carlo to calculate the UWFO for the CSL wave functions. The hopping parameters are set as $|t_1/t_0| = 0.5$

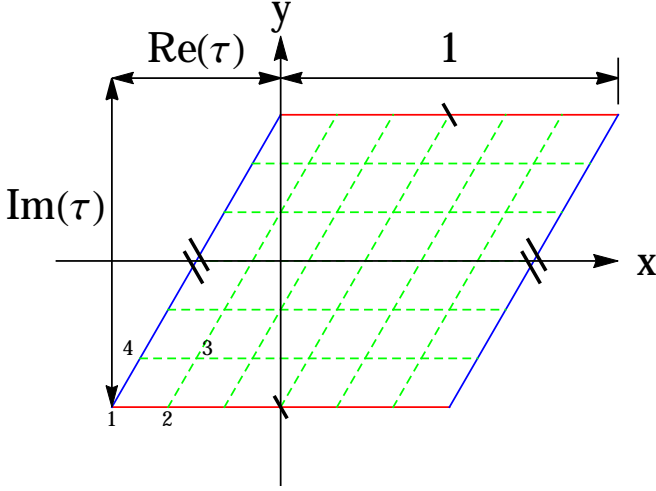


FIG. 1. The lattice system can be put on a torus by imposing the equivalence conditions: $z \sim z + 1$ and $z \sim z + \tau$ where $\tau = \tau_x + i\tau_y$ is a complex number. The principal region of a torus is bounded by the four points $z = \frac{1}{2}(\pm 1 \pm \tau)$. Here the top and bottom, left and right sides are identified, respectively.

for the CSL on the π -flux square lattice, where t_0 and t_1 for nearest neighbor and next nearest neighbor links, respectively. Since C_4 symmetry, the overlap \hat{S} in Eq. (1) has a vanishing exponent $\alpha_S = 0$. \hat{T} in Eq. (1) has the relatively small non-universal complex exponent $\alpha_T = 0.04208 + 0.07654i$ and the direct numeric computation is carried out on relatively large systems up to 12×12 lattice size in this paper. The CSL is the lattice analogy of $\nu = \frac{1}{2}$ bosonic Laughlin state^{31,32}. The parent Hamiltonians for CSL are also proposed in Refs.35 and 36. Our numerical results confirm the analogy by directly extracting the modular S and T matrices from the UWFO.

In the parton construction, the $S = \frac{1}{2}$ spin operator is written in terms of fermionic parton operators, $S^a(z_i) = \frac{1}{2}f_{\sigma}^{\dagger}(z_i)\sigma_{\sigma\sigma'}^a f_{\sigma'}(z_i)$. Here σ^a ($a = x, y, z$) is the Pauli matrices and $f_{i\sigma}$ ($\sigma = \uparrow / \downarrow$) is the fermionic parton operator. We take the complex variables for the i -site coordinate, $z_i = x_i + iy_i$, on a lattice. We have to impose the one-particle-per-site constraint for the partons, $f_{\uparrow}^{\dagger}(z_i)f_{\uparrow}(z_i) + f_{\downarrow}^{\dagger}(z_i)f_{\downarrow}(z_i) = 1$, such that the fermionic partons have the same Hilbert space on i -site as the spin operators $S^a(z_i)$. The GPWF for the spin system can be read as

$$|\Psi\rangle = \sum_{\{z_i\}} \mathcal{P}_G \Psi(\{z_i^{\uparrow}, z_i^{\downarrow}\}) |\{z_i\}\rangle, \quad (2)$$

where $|\{z_i\}\rangle$ the spin configuration and \mathcal{P}_G is the Gutzwiller projection operator to impose the one-particle-per-site constraint for the fermionic partons.

The GPWF can be put on a torus by implying the equivalence conditions: $z \sim z + 1$ and $z \sim z + \tau$, as shown in Fig. 1. The principal region of a torus is bounded by

the four points $z = \frac{1}{2}(\pm 1 \pm \tau)$. The torus is defined by two primitive vectors $\vec{\omega}_1 = 1$ and $\vec{\omega}_2 = \tau_x + i\tau_y$. The shape of the torus is invariant under the $SL(2, \mathbb{Z})$ transformations $\begin{pmatrix} \vec{\omega}'_1 \\ \vec{\omega}'_2 \end{pmatrix} = M \begin{pmatrix} \vec{\omega}_1 \\ \vec{\omega}_2 \end{pmatrix}$ with $M \in SL(2, \mathbb{Z})$ and the generators (\hat{S} and \hat{T}) have the expressions

$$\hat{S} = \begin{pmatrix} 0 & -1 \\ 1 & 0 \end{pmatrix}, \quad \hat{T} = \begin{pmatrix} 1 & 1 \\ 0 & 1 \end{pmatrix}. \quad (3)$$

Two different constructions of GPWF for a CSL in the lattice analogy of $\nu = \frac{1}{2}$ bosonic Laughlin state can be found in Refs. 31 and 32. In Ref. 32, the parton wave functions are discretized integer quantum Hall states and we call it *ideal* GPWF for a CSL. On a torus, we can explicitly write down the ideal GPWF in terms of the Laughlin-Jastrow wave functions³⁷

$$\begin{aligned} \mathcal{P}_G \Psi(\{z_i^{\uparrow}, z_i^{\downarrow}\}) &= e^{i\frac{K^{\uparrow}-K^{\downarrow}}{2}(Z^{\uparrow}-Z^{\downarrow})} \\ &\times \vartheta_{\frac{1}{2}, \frac{1}{2}}(Z^{\uparrow} - Z_0^{\uparrow} | \tau) \vartheta_{\frac{1}{2}, \frac{1}{2}}(Z^{\downarrow} - Z_0^{\downarrow} | \tau) \\ &\times \mathcal{P}_G \prod_{i < j}^N \vartheta_{\frac{1}{2}, \frac{1}{2}}(z_i^{\uparrow} - z_j^{\uparrow} | \tau) \prod_{k < l}^N \vartheta_{\frac{1}{2}, \frac{1}{2}}(z_k^{\downarrow} - z_l^{\downarrow} | \tau), \end{aligned} \quad (4)$$

where $\theta_{a,b}(z|\tau)$ is the theta function and $Z^{\sigma} = \sum_i z_i^{\sigma}$ is the center-of-mass coordinate. Different ground states are specified by the different zeros, Z_0^{σ} , in the center-of-mass wave functions. The zeros are determined by the general boundary conditions.^{37,38} The modular S and T matrices for the ideal GPWF in Eq.(4) can be analytically calculated by deformation the mass matrix¹⁴

$$S = \frac{1}{\sqrt{2}} \begin{pmatrix} 1 & 1 \\ 1 & -1 \end{pmatrix}, T = e^{-i\frac{2\pi c}{24}} \begin{pmatrix} 1 & 0 \\ 0 & e^{i\frac{\pi}{2}} \end{pmatrix}. \quad (5)$$

with the central charge $c = 1$, the same as those for the $\nu = \frac{1}{2}$ bosonic Laughlin state.

In Ref. 31, the *generic* GPWF for a CSL is written as

$$\mathcal{P}_G \Psi(\{z_i^{\uparrow}, z_i^{\downarrow}\}) = \mathcal{P}_G \det \varphi_i(z_j^{\uparrow}) \det \varphi_k(z_l^{\downarrow}), \quad (6)$$

where $\det \varphi_i(z_j^{\uparrow/\downarrow})$ is the determinate wave function for the fermionic partons filling the valence bands of the tight binding model

$$H_{\text{MF}} = - \sum_{ij, \sigma} t(z_i, z_j) f_{\sigma}^{\dagger}(z_i) f_{\sigma}(z_j) + \text{H.C.}, \quad (7)$$

on the π -flux square lattice with both nearest neighbor and next nearest neighbor hopping amplitude.³¹ There are $\frac{\pi}{2}$ flux in every triangle in the plaquette, e.g. Δ_{123} in \square_{1234} in Fig. 1, $\Phi(\Delta_{123}) = \arg(t_{z_1 z_2} t_{z_2 z_3} t_{z_3 z_1}) = \frac{\pi}{2}$. Different ground state wave functions can be obtained by different general boundary conditions. For the spin operator, the boundary condition is

$$S^+(z_i + 1) = e^{i\Phi_1^S} S^+(z_i), \quad S^+(z_i + \tau) = e^{i\Phi_2^S} S^+(z_i).$$

Due to fractionalization in the GPWF^{39,40}, the parton has the boundary condition

$$f_{\sigma}^{\dagger}(z_i + 1) = e^{i\frac{\sigma}{2}\Phi_1^S} f_{\sigma}^{\dagger}(z_i), \quad f_{\sigma}^{\dagger}(z_i + \tau) = e^{i\frac{\sigma}{2}\Phi_2^S} f_{\sigma}^{\dagger}(z_i),$$

with $\sigma = \pm 1$ for $f_{\uparrow/\downarrow}^\dagger$. When we increase $\Phi_{1,2}^s$ from 0 to 2π , the spin operators is invariant, however, the parton wave functions do not go back to themselves and lead to another ground state for GPWF. Therefore, we have different ground states for a CSL labeled by the spin fluxes in the holes of a torus $|\Phi_1^s, \Phi_2^s\rangle$,

$$\{|\Psi_a\rangle\} = \{|0,0\rangle, |0,2\pi\rangle, |2\pi,0\rangle, |2\pi,2\pi\rangle\}, \quad (8)$$

with $a = 1, 2, 3, 4$. Actually only two of them are linearly independent.

For the generic GPWF in Eq. (6), we use the UWFO in Eq. (1) to exact the modular matrices S and T . To carry out the UWFO, we need calculate the following overlaps

$$P_{ab} = \langle \Psi_a | \Psi_b \rangle, \quad \tilde{S}_{ab} = \langle \Psi_a | \Psi_b^S \rangle, \quad \tilde{T}_{ab} = \langle \Psi_a | \Psi_b^T \rangle. \quad (9)$$

where $|\Psi_a\rangle$ is the sate in Eq. (8) and $|\Psi_b^S\rangle = \hat{S}|\Psi_b\rangle$, $|\Psi_b^T\rangle = \hat{T}|\Psi_b\rangle$, where \hat{S} and \hat{T} are the 90° rotation and Dehn twist transformations in Eq. (3) on a torus. The P matrix has rank 2 with the numerical tolerance less than 10^{-3} implying two-fold ground state degeneracy.

Given GPWFs, we implement the “sign trick”⁴¹ to calculate the overlap

$$\begin{aligned} \langle \Psi_a | \Psi_b \rangle &= \sum_{\{z_i\}} \psi_a^*(\{z_i\}) \psi_b(\{z_i\}) \\ &\equiv \langle \Psi_a | \Psi_b \rangle_{\text{Amp}} \langle \Psi_a | \Psi_b \rangle_{\text{Sign}} \end{aligned} \quad (10)$$

where $\psi_a(\{z_i\})$ is the amplitude wave function of the spin configuration $\{z_i\}$ in $|\Psi_a\rangle$ and the sign term

$$\langle \Psi_a | \Psi_b \rangle_{\text{Sign}} = \sum_{\{z_i\}} \rho_{ab} \frac{\psi_a^*(\{z_i\}) \psi_b(\{z_i\})}{|\psi_a(\{z_i\}) \psi_b(\{z_i\})|} \quad (11)$$

is calculated by Monte Carlo method according to the weight $\rho_{ab} = |\psi_a(\{z_i\}) \psi_b(\{z_i\})|$. The amplitude term is the normalization factor for weight ρ_{ab}

$$\langle \Psi_a | \Psi_b \rangle_{\text{Amp}} = \sum_{\{z_i\}} |\psi_a(\{z_i\}) \psi_b(\{z_i\})|. \quad (12)$$

Actually, we are only interested in the ratios of amplitudes. For example, for P matrix in Eq. (9), we evaluate the matrix-element amplitude ratios

$$\frac{\langle \Psi_a | \Psi_b \rangle_{\text{Amp}}}{\langle \Psi_1 | \Psi_1 \rangle_{\text{Amp}}} = \frac{\sum_{\{z_i\}} \rho_{ab;11} \sqrt{|\frac{\psi_a(\{z_i\}) \psi_b(\{z_i\})}{\psi_1(\{z_i\}) \psi_1(\{z_i\})}|}}{\sum_{\{z_i\}} \rho_{ab;11} \sqrt{|\frac{\psi_1(\{z_i\}) \psi_1(\{z_i\})}{\psi_a(\{z_i\}) \psi_b(\{z_i\})}|}} \quad (13)$$

according to the Monte Carlo sampling weight $\rho_{ab;11} = \sqrt{|\psi_a(\{z_i\}) \psi_b(\{z_i\}) \psi_1(\{z_i\}) \psi_1(\{z_i\})|}$.

We set the mean field hopping parameters as $t_1/t_0 = 0.5$, where t_0 and t_1 are for nearest neighbor and next nearest neighbor links, respectively. The overlap calculations are carried out on the systems with $L \times L$ lattice sizes, $L = 6, 8, 10, 12$. From the overlaps in Eq. (9), we follow the steps below to extract the modular S and T matrices. We first digonalize the P matrix

$$P = U^\dagger P_\Lambda U, \quad U = (u_1, u_2, u_3, u_4). \quad (14)$$

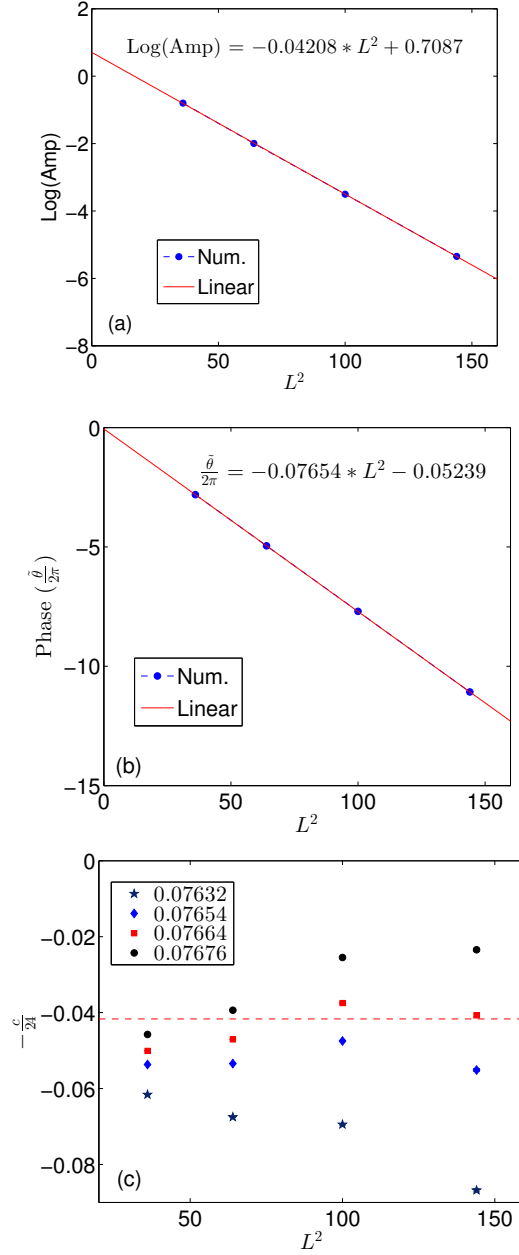


FIG. 2. L^2 -dependent of amplitude and phase of T' in Eq. (16) are shown in (a) and (b), respectively. Here $\text{Log}(\text{Amp}) \equiv \log(|T'_{11}|)$ and $\frac{\hat{\theta}}{2\pi} \equiv \frac{\arg T'_{11}}{2\pi} + k$ with $k = 3, 5, 8, 11$ for $L = 6, 8, 10, 12$. In (c), we plot $-\frac{c}{24} = \frac{\arg(T'_{11})}{2\pi} + \frac{\text{Im}(\alpha_T)}{2\pi} L^2 \pmod{1}$ with different $\frac{\text{Im}(\alpha_T)}{2\pi} = 0.07632, 0.07654, 0.07664, 0.07676$. The red dashed line is for $c = 1$. In (c), the numerical error bars are included and smaller than the symbols' sizes.

Only two eigenvectors (e.g. u_3 and u_4) have non-zero eigenvalues around 2. These two states (u_3 and u_4) are the linearly independent ground sates. In terms of the normalized $\tilde{U} = (u_3, u_4)$, the overlaps for \tilde{S} and \tilde{T} in Eq.

(9) turn out to be 2×2 square matrices

$$S_{2 \times 2}^1 = \tilde{U}^\dagger \tilde{S}_{4 \times 4} \tilde{U}, \quad T_{2 \times 2}^1 = \tilde{U}^\dagger \tilde{T}_{4 \times 4} \tilde{U}. \quad (15)$$

Generally, T^1 is not diagonal since u_3 and u_4 are not the minimum entangled states or eigenstates of the Wilson loop operators²¹. We then diagonalize T_1 to obtain the minimum entangled states v_1 and v_2

$$T^1 = V^\dagger T' V, \quad S^1 = V^\dagger S' V, \quad V = (v_1, v_2), \quad (16)$$

where T' is diagonal and the phases of V are fixed according to the conditions $S'_{12} = S'_{21}$ and $S'_{1i} > 0$.

Since the CSL wave function has the 90° rotation symmetry, the exponent in S' in Eq.(16) vanishes, $\alpha_S = 0$, that is confirmed in the numerical calculations. The UWFO of the T matrix has a complex exponent α_T in the prefactor. The real part of the exponent $\text{Re}(\alpha_T)$ is easily obtained from the amplitude of the T' in Eq.(16) by fitting $\text{Log}(\text{Amp}) \equiv \log(|T'_{11}|)$ with respect to L^2 , $\text{Re}(\alpha_T) = 0.04208$, as shown in Fig. 2 (a). The phase $\tilde{\theta}$ is defined up 2π , $\frac{\tilde{\theta}}{2\pi} \equiv \frac{\arg(T'_{11})}{2\pi} + k = -\frac{\text{Im}(\alpha_T)}{2\pi} L^2 - \frac{c}{24}$ with $k \in \mathbb{Z}$. For $L = 6, 8, 10, 12$, the corresponding integers are $k = 3, 5, 8, 11$. From the fitting in Fig. 2 (b), we obtain $\text{Im}(\alpha_T) = 0.4809$. The central charge is sensitive to the exact value of $\text{Im}(\alpha_T)$ as shown in Fig. 2 (c). The final result for the modular S and T matrices is

$$S = \begin{pmatrix} 0.714 & 0.707 \\ 0.707 & -0.698 \end{pmatrix}, \quad T = e^{-i\frac{2\pi c}{24}} \begin{pmatrix} 1 & 0 \\ 0 & e^{i0.501\pi} \end{pmatrix} \quad (17)$$

with the central charge $c \simeq 1.25 \pm 0.5$, very close to the exact result for the ideal GPWF in Eq. (5).

Above we apply the UWFO method on the square lattice. For a general Bravais lattice, we can firstly map it onto an equivalent square lattice. We take the kagome lattice as example. We map the unit cell of the kagome lattice onto the one with square unit cell. Different sites within the unit cell are mapped onto different orbitals on the square lattice, as shown in Fig.3. Then we can make the modular transformations \hat{S} and \hat{T} on the square lattice torus. **For systems without 90° rotation symmetry, the exponents $\alpha_{S,T}$ in Eq. (1) are both finite.** On the square lattice, we can also use Kadanoff block renormalization procedure to reduce the system size $L^2 \rightarrow \tilde{L}^2$. Then the exponents in the prefactors of UWFO can be

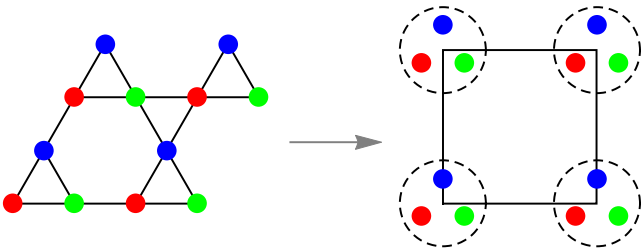


FIG. 3. Kagome lattice is mapped onto a square lattice with three orbitals per site.

significantly reduced. Many local unitary transformations on the lattice can potentially reduce the exponents in the UWFO. If different ground state sectors have the same topological spins, we can follow Ref. 15 to identify the minimum entangled states to diagonalize the modular T matrix. The UWFO method is easily generalized to the 3+1D topological orders in the GPWFs. The GPWF for quantum dimer models in 3D has already been constructed in Ref. 42. In 3D, the modular group of the 3-torus is $SL(3, \mathbb{Z})$ generated by

$$\hat{S} = \begin{pmatrix} 0 & 1 & 0 \\ 0 & 0 & 1 \\ 1 & 0 & 0 \end{pmatrix}, \quad \hat{T} = \begin{pmatrix} 1 & 0 & 0 \\ 1 & 1 & 0 \\ 0 & 0 & 1 \end{pmatrix}. \quad (18)$$

We can use the UWFO to directly study the topological information in 3+1D¹⁶.

In conclusion, we use the universal wave function overlap method to exact the modular S and T matrices for the topological order in the Gutzwiller-projected parton wave function for the chiral spin liquid state on the square lattice. The chiral spin liquid is the lattice analogy of $\nu = \frac{1}{2}$ bosonic Laughlin state and the analogy is directly confirmed by the modular S and T matrices from the universal wave function overlap. The exponents in the prefactors of the wave function overlaps are found to be small and the variational Monte Carlo calculations are carried out on relatively large systems. The Monte Carlo calculations of the universal wave function overlap can be easily generalize to other Bravais lattices and 3+1D topological orders.

X-G. W is supported by NSF Grant No. DMR-1005541 and NSFC 11274192. He is also supported by the BMO Financial Group and the John Templeton Foundation. Research at Perimeter Institute is supported by the Government of Canada through Industry Canada and by the Province of Ontario through the Ministry of Research.

-
- ¹ X. G. Wen, International Journal of Modern Physics B **04**, 239 (1990).
 - ² X. G. Wen, Phys. Rev. B **40**, 7387 (1989).
 - ³ X. G. Wen and Q. Niu, Phys. Rev. B **41**, 9377 (1990).
 - ⁴ M. Levin and X.-G. Wen, Phys. Rev. Lett. **96**, 110405 (2006).
 - ⁵ A. Kitaev and J. Preskill, Phys. Rev. Lett. **96**, 110404 (2006).
 - ⁶ X. Chen, Z.-C. Gu, and X.-G. Wen, Phys. Rev. B **82**, 155138 (2010).
 - ⁷ X. Wen, *Quantum Field Theory of Many-Body Systems: From the Origin of Sound to an Origin of Light and Electrons*, Oxford Graduate Texts (OUP Oxford, 2004).
 - ⁸ R. B. Laughlin, Phys. Rev. Lett. **50**, 1395 (1983).
 - ⁹ F. Wilczek and A. Zee, Phys. Rev. Lett. **52**, 2111 (1984).
 - ¹⁰ D. Arovas, J. R. Schrieffer, and F. Wilczek, Phys. Rev. Lett. **53**, 722 (1984).
 - ¹¹ X.-G. Wen, International Journal of Modern Physics B **6**, 1711 (1992).
 - ¹² X.-G. Wen, Advances in Physics **44**, 405 (1995).
 - ¹³ E. Keski-Vakkuri and X.-G. Wen, International Journal of Modern Physics B **07**, 4227 (1993).
 - ¹⁴ X.-G. Wen, ArXiv e-prints (2012), arXiv:1212.5121 [cond-mat.str-el].
 - ¹⁵ F. Liu, Z. Wang, Y.-Z. You, and X.-G. Wen, ArXiv e-prints (2013), arXiv:1303.0829 [cond-mat.str-el].
 - ¹⁶ H. Moradi and X.-G. Wen, ArXiv e-prints (2014), arXiv:1401.0518 [cond-mat.str-el].
 - ¹⁷ H. He, H. Moradi, and X.-G. Wen, ArXiv e-prints (2014), arXiv:1401.5557 [cond-mat.str-el].
 - ¹⁸ Z. Wang, American Mathematical Society, Providence, RI (2010).
 - ¹⁹ E. Verlinde, Nuclear Physics B **300**, 360 (1988).
 - ²⁰ I. Affleck, Phys. Rev. Lett. **56**, 746 (1986).
 - ²¹ Y. Zhang, T. Grover, A. Turner, M. Oshikawa, and A. Vishwanath, Phys. Rev. B **85**, 235151 (2012).
 - ²² L. Cincio and G. Vidal, Phys. Rev. Lett. **110**, 067208 (2013).
 - ²³ H.-H. Tu, Y. Zhang, and X.-L. Qi, Phys. Rev. B **88**, 195412 (2013).
 - ²⁴ M. P. Zaletel, R. S. K. Mong, and F. Pollmann, Phys. Rev. Lett. **110**, 236801 (2013).
 - ²⁵ W. Zhu, D. N. Sheng, and F. D. M. Haldane, Phys. Rev. B **88**, 035122 (2013).
 - ²⁶ Y. Zhang and X.-L. Qi, Phys. Rev. B **89**, 195144 (2014).
 - ²⁷ Y. Tserkovnyak and S. Simon, Phys. Rev. Lett. **90**, 016802 (2003).
 - ²⁸ E. Kapit, P. Ginsparg, and E. Mueller, Phys. Rev. Lett. **108**, 066802 (2012).
 - ²⁹ Y.-L. Wu, B. Estienne, N. Regnault, and B. A. Bernevig, Phys. Rev. Lett. **113**, 116801 (2014).
 - ³⁰ L.-Y. Hung and X.-G. Wen, Phys. Rev. B **89**, 075121 (2014).
 - ³¹ X. G. Wen, F. Wilczek, and A. Zee, Phys. Rev. B **39**, 11413 (1989).
 - ³² V. Kalmeyer and R. B. Laughlin, Phys. Rev. Lett. **59**, 2095 (1987).
 - ³³ X. G. Wen, Phys. Rev. B **44**, 2664 (1991).
 - ³⁴ X.-G. Wen, Phys. Rev. B **60**, 8827 (1999).
 - ³⁵ D. Schroeter, E. Kapit, R. Thomale, and M. Greiter, Phys. Rev. Lett. **99**, 097202 (2007).
 - ³⁶ H. Yao and S. Kivelson, Phys. Rev. Lett. **99**, 247203 (2007).
 - ³⁷ F. D. M. Haldane and E. H. Rezayi, Phys. Rev. B **31**, 2529 (1985).
 - ³⁸ Q. Niu, D. J. Thouless, and Y.-S. Wu, Phys. Rev. B **31**, 3372 (1985).
 - ³⁹ J.-W. Mei and X.-G. Wen, ArXiv e-prints (2014), arXiv:1407.0869 [cond-mat.str-el].
 - ⁴⁰ Z.-X. Liu, J.-W. Mei, P. Ye, and X.-G. Wen, ArXiv e-prints (2014), arXiv:1408.1676 [cond-mat.str-el].
 - ⁴¹ Y. Zhang, T. Grover, and A. Vishwanath, Phys. Rev. B **84**, 075128 (2011).
 - ⁴² V. Ivanov, Y. Qi, and L. Fu, Phys. Rev. B **89**, 085128 (2014).